Water Splitting

DOI: 10.1002/anie.201000664

A Coupling Strategy to Produce Hydrogen and Ethylene in a Membrane Reactor**

Heqing Jiang, Zhengwen Cao, Steffen Schirrmeister, Thomas Schiestel, and Jürgen Caro**

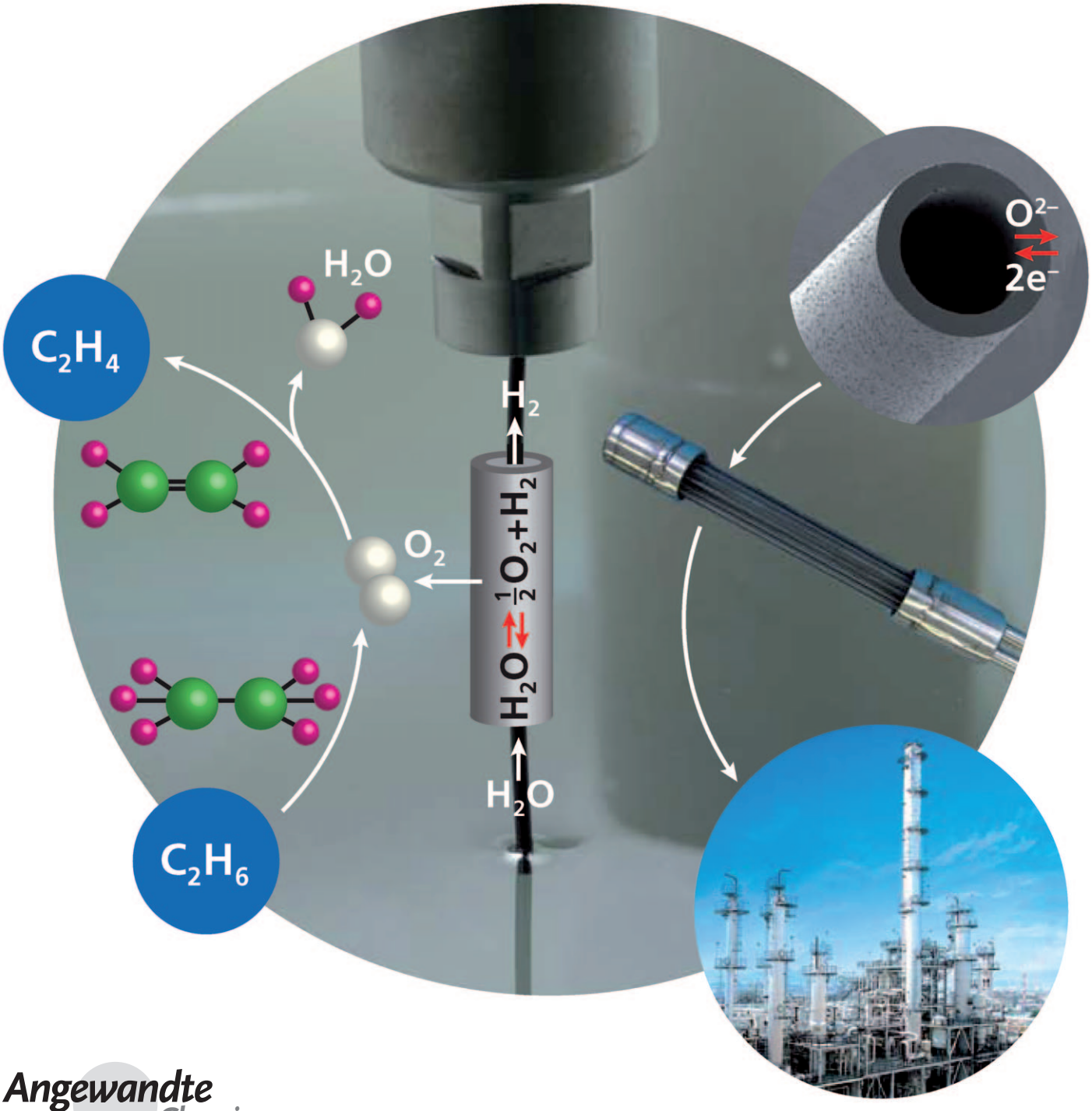

Following the concept of process intensification,[1,2] the effective coupling of two chemical reactions in one apparatus is gaining increasing interest from both academia and industry.[3–5] In the past years, most of theses studies have focused on the combination of an endothermic dehydrogenation with an exothermic hydrogenation of hydrocarbons in a Pd membrane reactor.[6,7] This coupled dehydrogenation/hydrogenation has also been studied in fixed-bed reactors; for example, the simultaneous ethylbenzene dehydrogenation and benzene hydrogenation.[8] Recently, Kondratenko et al. reported the production of ethylene with the simultaneous, almost 100% removal of nitrous oxide (N_2O) by coupling the N_2O decomposition with the thermal dehydrogenation of ethane in a catalytic fixed-bed reactor.[9] However, by the coupling of the two reactions in the fixed-bed reactor, a subsequent procedure is necessary to separate the products. If the reactions are conducted in a membrane reactor, the products will be kept separated on the two sides of the membrane. Therefore, it appears attractive to search for new pairs of industrially interesting reactions in membrane reactors.

Hydrogen production from water splitting has attracted much attention in the past decades because hydrogen is considered a promising alternative to fossil fuels.[10,11] One technique to enhance the hydrogen production rate from the equilibrium-limited water splitting reaction is the in situ removal of the oxygen that is produced simultaneously using a mixed oxygen-ion and electron-conducting membrane.[12–16] Previous studies have shown that an operating temperature of 1683 °C was necessary to obtain a hydrogen production rate of 0.6 $cm^3 min^{-1} cm^{-2}$ in a mixed-conducting ZrO_2-TiO_2-Y_2O_3 membrane.[17] To lower the operating temperature, Balachandran et al. coupled water splitting with hydrogen combustion as a model reaction in a ceramic-metal membrane reactor, by feeding hydrogen to the permeate side to consume the permeated oxygen.[18] A maximum hydrogen production rate of 10.0 $cm^3 min^{-1} cm^{-2}$ was obtained at 900 °C as a proof of principle.

As the amount of hydrogen produced in this model reaction was equivalent to the amount of hydrogen consumed, we looked for practice-relevant coupled reactions in membrane reactors. Recently, we reported the coupling of water splitting with partial oxidation of methane for the simultaneous production of hydrogen and synthesis gas (a mixture of CO and H_2) at temperatures of between 850 to 950 °C in a perovskite $BaCo_xFe_yZr_{1-x-y}O_{3-\delta}$ (BCFZ) hollow-fiber membrane reactor.[19] The BCFZ hollow-fiber membrane shows a high oxygen permeation rate and has been used for the production of oxygen-enriched air and the abatement of nitrogen oxides.[20–22]

Herein, we combine water splitting and ethane dehydrogenation in a BCFZ oxygen-permeable membrane reactor at moderate temperatures (700–800 °C). Figure 1 shows the concept of water splitting coupled with the dehydrogenation

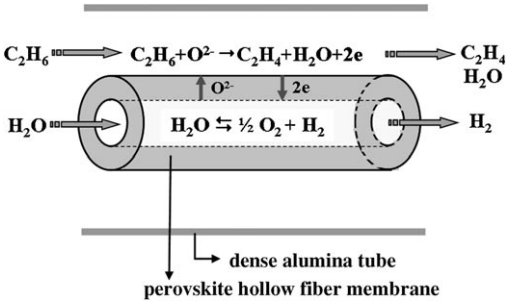

Figure 1. Water splitting coupled with ethane dehydrogenation in a perovskite oxygen-permeable membrane reactor.

of ethane in the perovskite hollow fiber membrane reactor. First, water dissociates into hydrogen and oxygen on the core side of the perovskite BCFZ membrane. The produced oxygen is then removed as oxygen ions (O^{2-}) to the ethane side of the membrane, where it is consumed to convert ethane into ethylene according to $C_2H_6 + O^{2-} \rightarrow C_2H_4 + H_2O + 2e^-$. Local charge neutrality is maintained by the counter-diffusion of electrons. Thus, the produced oxygen can be continuously removed via the BCFZ membrane, and more hydrogen from water splitting can be produced even under equilibrium-controlled conditions. Ethylene can be obtained simultaneously after steam condensation on the shell side of the membrane. The advantage of this coupling strategy is that the hydrogen produced from water splitting and the ethylene that forms from ethane dehydrogenation are inherently separated in the membrane reactor.

Experimentally, it was found that the hydrogen production rate from water splitting on the core side is very low (<0.025 $cm^3 min^{-1} cm^{-2}$) at temperatures below 950 °C if only the inert sweep gas helium was applied on the shell side of the BCFZ hollow-fiber membrane to reduce the oxygen partial pressure.[19] However, significant amounts of hydrogen were obtained on the steam side even at moderate temperatures (700–800 °C) upon coupling of the water dissociation with the ethane dehydrogenation. As shown in Figure 2a, by feeding 7.5 vol% C_2H_6 to the shell side, the hydrogen production rate from water splitting increases from 0.1 to 0.4 $cm^3 min^{-1} cm^{-2}$ when the temperature rises from 700 to 800 °C. With rising temperature, the equilibrium of the endothermic water

[*] Dr. H. Jiang, Z. Cao, Prof. Dr. J. Caro
Institute of Physical Chemistry and Electrochemistry
Leibniz University of Hannover
Callinstrasse 3A, 30167 Hannover (Germany)
Fax: (+49) 511-7621-9121
E-mail: heqing.jiang@pci.uni-hannover.de
juergen.caro@pci.uni-hannover.de
Dr. S. Schirrmeister
Uhde GmbH
Friedrich-Uhde-Strasse 15, 44141 Dortmund (Germany)
Dr. T. Schiestel
Fraunhofer Institute of Interfacial Engineering and Biotechnology (IGB), Nobelstr. 12, 70569 Stuttgart (Germany)

[**] The authors gratefully acknowledge the financial support of the BMBF for the project 03C0343A SynMem under the auspices of ConNeCat (Competence Network Catalysis). A. Feldhoff and F. Steinbach are thanked for support in electron microscopy.

Supporting information for this article is available on the WWW under http://dx.doi.org/10.1002/anie.201000664.

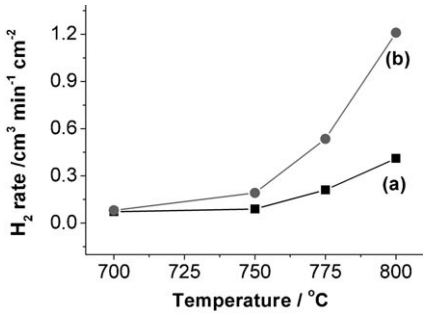

Figure 2. H_2 production rate on the core side as a function of temperature. Core side: $F_{H_2O} = 30\ cm^3\ min^{-1}$, $F_{He} = 10\ cm^3\ min^{-1}$; shell side: $F_{total} = 40\ cm^3\ min^{-1}$ with an ethane concentration of a) 7.5% and b) 20%.

splitting is shifted towards oxygen and hydrogen as products. Moreover, the oxygen permeation rate of the BCFZ membrane increased with increasing temperature, according to Wagner theory.[23,24] The fast removal of the oxygen produced from water splitting causes further water to dissociate, and thus the equilibrium constraint for the hydrogen production is overcome.

Apart from operating temperature and membrane thickness, according to Wagner theory[23,24] the oxygen permeation rate is related to the oxygen partial-pressure gradient across the membrane. By feeding more ethane to the shell side of the BCFZ membrane, a larger driving force was provided for the fast removal of oxygen from the steam side, thus increasing the hydrogen production rate. Figure 2 presents the temperature dependence of the hydrogen production rate upon feeding 7.5 vol% (a) and 20 vol% ethane (b) to the shell side. The hydrogen production rate in case (b) is always higher than for (a) at all temperatures investigated; the hydrogen production rate reaches $1.2\ cm^3\ min^{-1}\ cm^{-2}$ at 800°C (Figure 2b).

The permeated oxygen from water splitting can be utilized for the oxidative dehydrogenation of ethane (ODE) to ethylene on the shell side of the membrane. As shown in Table 1, the ethane conversion increased from 6% to 59% and the ethylene selectivity increased from 67% to 89% upon increasing the temperature from 700 to 800°C. At 700°C, only a very small amount of hydrogen is detected on the shell side (<0.15% H_2), indicating that the ODE process ($C_2H_6 + O^{2-} \rightarrow C_2H_4 + H_2O + 2e^-$) dominates over the thermal dehydrogenation of ethane (TDE; $C_2H_6 \rightleftarrows C_2H_4 + H_2$). Because only traces of CO_x were detected, and the permeated oxygen mainly reacted with hydrogen forming water, the amount of water produced on the shell side can be estimated based on the difference of flow rates between H_2 and C_2H_4 at the exit. The rate of water produced on the shell side is $0.06\ cm^3\ min^{-1}\ cm^{-2}$ at 700°C and $0.5\ cm^3\ min^{-1}\ cm^{-2}$ at 800°C, which is almost equal to that of water consumed on the core side. At 800°C, the TDE process cannot be neglected, and it occurs parallel to the ODE process.[25–27] Consequently, ethylene, hydrogen, water, and non-reacted ethane were present on the shell side, and the ethylene yield is about 55% at 800°C. As a control experiment, the dehydrogenation of ethane in the presence of water was also investigated in a fixed-bed reactor filled with BCFZ perovskite. At 800°C, an ethylene yield of 47% was obtained with an ethylene selectivity of 71% in the fixed-bed reactor (see the Supporting Information, Table S1). Obviously, more ethylene was obtained based on the coupling strategy in BCFZ membrane reactor.

Figure 3 presents the simultaneous production of hydrogen and ethylene in the BCFZ hollow-fiber membrane reactor as a function of time. During a period of 100 h, about 60% ethane conversion and 90% ethylene selectivity were obtained. Simultaneously, the hydrogen production rate on the steam side reaches $0.8\ cm^3\ min^{-1}\ cm^{-2}$. The BCFZ hollow-fiber membrane is still gas-tight after 100 h, at which time we stopped the test.

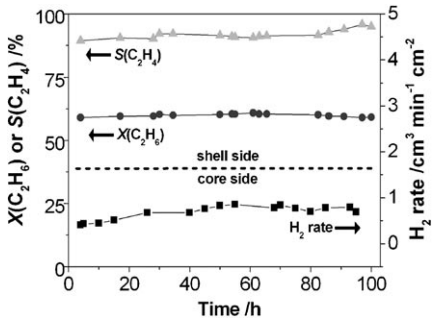

Figure 3. 100 h operation for H_2 production on the core side and the simultaneous ethylene production on the shell side at 800°C. Core side: $F_{H_2O} = 30\ cm^3\ min^{-1}$, $F_{He} = 10\ cm^3\ min^{-1}$; shell side: $40\ cm^3\ min^{-1}$ ($F_{C_2H_6} = 3\ cm^3\ min^{-1}$, $F_{He} = 36\ cm^3\ min^{-1}$, $F_{Ne} = 1\ cm^3\ min^{-1}$).

Table 1: Ethane conversion $X(C_2H_6)$ and ethylene selectivity $S(C_2H_4)$ on the shell side of BCFZ membrane at different temperatures.[a]

T [°C]	$X(C_2H_6)$ [%]	$S(C_2H_4)$ [%]
700	6	67
750	20	89
775	37	88
800	59	89

[a] Core side: $40\ cm^3\ min^{-1}$ ($F_{H_2O} = 30\ cm^3\ min^{-1}$, $F_{He} = 10\ cm^3\ min^{-1}$). Shell side: $40\ cm^3\ min^{-1}$ ($F_{C_2H_6} = 3\ cm^3\ min^{-1}$, $F_{He} = 36\ cm^3\ min^{-}$, $F_{Ne} = 1\ cm^3\ min^{-1}$).

Scanning electron microscopy was used to characterize the used hollow fiber. Although the membrane surface was eroded on the ethane side, there was no development of cracks in the central dense part of the membrane. In contrast to layered porous membranes,[28,29] the BCFZ dense membrane only allows the transport of oxygen ions with infinite selectivity, and therefore there is no permeation of other gases, including water, through the membrane.[13,22] Figure 4a shows the cross-section of the used BCFZ hollow fiber with an eroded layer of about 10 μm on the membrane surface exposed to the ethane side. Small particles of 0.2–1.0 μm were well-dispersed on the membrane surface (Figure 4b,c).

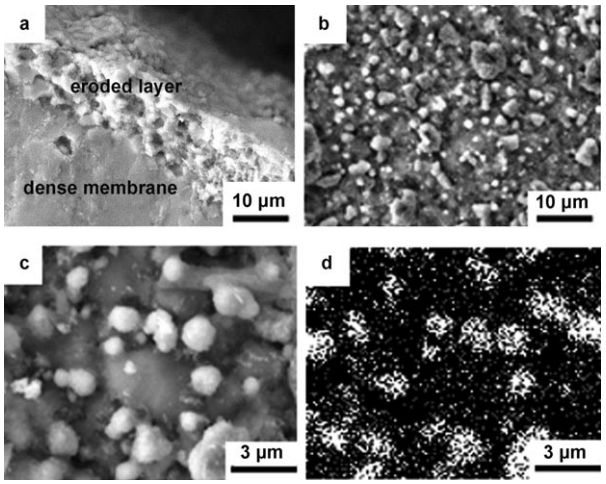

Figure 4. SEM images of the ethane side of the BCFZ hollow-fiber membrane after measurement and 100 h operation (see Figure 3). a) Cross-section, b,c) top views, and d) the corresponding elemental distribution image of cobalt.

Energy-dispersive X-ray spectroscopy (EDXS; Figure 4d) indicates that the small particles are mainly composed of cobalt oxide. Cobalt extraction by reduction of cobalt cations from perovskite, resulting in cobalt-enriched surface particles, has been reported previously.[30] Here, owing to the reducing ethane/ethylene atmosphere, cobalt cations of the perovskite BCFZ lattice might be partly reduced, leading to the formation of the surface eroded layer with the thickness of about 10 μm.

Hydrogen can also be produced from water by electrolysis or photocatalysis.[31–33] Water electrolysis is commercially available today for small-scale hydrogen production; the main obstacle in commercial exploitation of this technology for large-scale hydrogen production is the high cost of electricity and the noble metal catalysts.[31,32] The main feature of photoelectrolysis and the photocatalytic process is the use of solar energy. Current research efforts involve overcoming the low efficiency and the unsatisfactory stability.[32,33] Compared to the water splitting by electrolysis or photocatalysis, the direct thermal hydrogen production would require heating water to above 2500 °C to obtain appreciable yields; the high temperature is difficult to reach and maintain from a materials perspective.

In conclusion, we demonstrate a novel coupling strategy to produce hydrogen and ethylene in a BCFZ hollow-fiber membrane reactor. By coupling water splitting and ethane dehydrogenation on the opposite sides of the oxygen-permeable membrane, not only was a hydrogen production rate of around 1.0 $cm^3 min^{-1} cm^{-2}$ achieved at 800 °C, but also an ethylene yield of around 55 % was obtained on the other side of the membrane. To the best of our knowledge, this is the first report on the coupling of water splitting and ethane dehydrogenation in a membrane reactor. The membrane-based hydrogen production from water splitting is still in its early stages, and more laboratory efforts should be given to improve the properties and membrane stability in the near future.

Experimental Section

The dense BCFZ hollow-fiber membranes were fabricated by phase-inversion spinning followed by sintering.[34] The sintered fiber had a wall thickness of around 0.17 mm with an outer diameter of 1.10 mm and an inner diameter of 0.76 mm. To obtain isothermal conditions, two ends of the fiber were coated by gold paste followed by sintering at 950 °C, and a dense gold film that is not permeable to oxygen was thus obtained. The length of the uncoated central part was 3 cm, and the effective membrane area was 0.86 cm^2. The measurements were carried out in a high-temperature reactor as described in our previous work.[19–21] Figure S1 in the Supporting Information shows a schematic diagram of the membrane reactor used in this work. The gold-coated hollow fiber was sealed by a silicon-rubber ring and the uncoated part that is permeable to oxygen was kept in the middle of the oven. H_2O diluted by He was fed to the core side and a mixture of C_2H_6, Ne, and He was fed to the shell side. C_2H_6, He, and Ne flow rates were controlled by gas mass-flow controllers (Bronkhorst). The H_2O flow rate was controlled by a liquid mass-flow controller (Bronkhorst) and was completely evaporated at 180 °C before it was fed to the reactor. All of the gas lines to the reactor and to the gas chromatograph were heated to 180 °C. The concentrations of the gases at the exit of the reactor were determined by an on-line gas chromatograph (Agilent 6890). Assuming that the oxygen from water splitting on the core side was totally removed and the flow rate at the outlet is equal to that at the inlet, and H_2 production rate on the core side was calculated from the total flow rate F_{core} ($cm^3 min^{-1}$), the hydrogen concentration $c(H_2)$, and the effective membrane area S (cm^2) according to Equation (1):

$$J(H_2) = \frac{F_{core}\, c(H_2)}{S} \tag{1}$$

The C_2H_6 conversion $X(C_2H_6)$ and the C_2H_4 selectivity $S(C_2H_4)$ were calculated with Equations (2) and (3), where $F(i)$ is the flow rate of species i on the shell of the hollow fiber membrane.

$$X(C_2H_6) = \left(1 - \frac{F(C_2H_6, \text{out})}{F(C_2H_6, \text{in})}\right) \times 100\,\% \tag{2}$$

$$S(C_2H_4) = \frac{F(C_2H_4, \text{out})}{F(C_2H_6, \text{in}) - F(C_2H_6, \text{out})} \times 100\,\% \tag{3}$$

The surface morphology of the used fiber was characterized using a field-emission scanning electron microscopy (SEM) of the type JEOL JSM-6700F. An energy dispersive X-ray (EDX) spectrometer of the type Oxford Instruments INCA-300 was used for the elemental analysis.

Received: February 3, 2010
Revised: March 22, 2010
Published online: June 10, 2010

Keywords: ethane dehydrogenation · hydrogen · membrane reactors · perovskite · water splitting

[1] S. A. Bhat, J. Sadhukhan, *AIChE J.* **2009**, *55*, 408 – 422.
[2] J. Pérez-Ramírez, B. Vigeland, *Angew. Chem.* **2005**, *117*, 1136 – 1139; *Angew. Chem. Int. Ed.* **2005**, *44*, 1112 – 1115.
[3] V. R. Choudhary, B. S. Uphade, S. A. R. Mulla, *Angew. Chem.* **1995**, *107*, 721 – 723; *Angew. Chem. Int. Ed. Engl.* **1995**, *34*, 665 – 666.
[4] R. C. Ramaswamy, P. A. Ramachandran, M. P. Dudukovic, *Chem. Eng. Sci.* **2008**, *63*, 1654 – 1667.
[5] J. H. Blank, J. Beckers, P. E. Collignon, F. Clerc, G. Rothenberg, *Chem. Eur. J.* **2007**, *13*, 5121 – 5128.
[6] T. M. Moustafa, S. S. E. H. Elnashaie, *J. Membr. Sci.* **2000**, *178*, 171 – 184.

[7] M. H. Khademi, A. Jahanmiri, M. R. Rahimpour, *Int. J. Hydrogen Energy* **2009**, *34*, 5091 – 5107.
[8] M. E. E. Abashar, *Chem. Eng. Proc.* **2004**, *43*, 1195 – 1202.
[9] E. V. Kondratenko, O. Ovsitser, *Angew. Chem.* **2008**, *120*, 3271 – 3273; *Angew. Chem. Int. Ed.* **2008**, *47*, 3227 – 3229.
[10] D. Lu, T. Takata, N. Saito, Y. Inoue, K. Domen, *Nature* **2006**, *440*, 295 – 297.
[11] O. Coskuner, E. A. A. Jarvis, T. C. Allison, *Angew. Chem.* **2007**, *119*, 7999 – 8001; *Angew. Chem. Int. Ed.* **2007**, *46*, 7853 – 7855.
[12] H. H. Wang, Z. Cong, W. S. Yang, *Chem. Commun.* **2002**, 1468 – 1469.
[13] J. Sunarso, S. Baumann, J. M. Serra, W. A. Meulenberg, S. Liu, Y. S. Lin, J. D. Costa, *J. Membr. Sci.* **2008**, *320*, 13 – 41.
[14] Y. T. Liu, X. Y. Tan, K. Li, *Catal. Rev. Sci. Eng.* **2006**, *48*, 145 – 198.
[15] C. Chen, S. J. Feng, S. Ran, D. C. Zhu, W. Liu, H. J. M. Bouwmeester, *Angew. Chem.* **2003**, *115*, 5354 – 5356; *Angew. Chem. Int. Ed.* **2003**, *42*, 5196 – 5198.
[16] J. Caro, K. J. Caspary, C. Hamel, B. Hoting, P. Kölsch, B. Langanke, K. Nassauer, T. Schiestel, A. Schmidt, R. Schomäcker, A. Seidel-Morgenstern, E. Tsotsas, I. Voigt, H. H. Wang, R. Warsitz, S. Werth, A. Wolf, *Ind. Eng. Chem. Res.* **2007**, *46*, 2286 – 2294.
[17] H. Naito, H. Arashi, *Solid State Ionics* **1995**, *79*, 366 – 370.
[18] U. Balachandran, T. H. Lee, S. E. Dorris, *Int. J. Hydrogen Energy* **2007**, *32*, 451 – 456.
[19] H. Q. Jiang, H. H. Wang, S. Werth, T. Schiestel, J. Caro, *Angew. Chem.* **2008**, *120*, 9481 – 9484; *Angew. Chem. Int. Ed.* **2008**, *47*, 9341 – 9344.
[20] H. Q. Jiang, L. Xing, O. Czuprat, H. H. Wang, S. Schirrmeister, T. Schiestel, J. Caro, *Chem. Commun.* **2009**, 6738 – 6740.
[21] H. Q. Jiang, H. H. Wang, F. Y. Liang, S. Werth, T. Schiestel, J. Caro, *Angew. Chem.* **2009**, *121*, 3027 – 3030; *Angew. Chem. Int. Ed.* **2009**, *48*, 2983 – 2986.
[22] H. H. Wang, S. Werth, T. Schiestel, J. Caro, *Angew. Chem.* **2005**, *117*, 7066 – 7069; *Angew. Chem. Int. Ed.* **2005**, *44*, 6906 – 6909.
[23] M. Schroeder, *Phys. Chem. Chem. Phys.* **2005**, *7*, 166 – 172.
[24] R. Merkle, J. Maier, H. J. M. Bouwmeester, *Angew. Chem.* **2004**, *116*, 5179 – 5183; *Angew. Chem. Int. Ed.* **2004**, *43*, 5069 – 5073.
[25] S. Gaab, M. Machli, J. Find, R. K. Grasselli, J. A. Lercher, *Top. Catal.* **2003**, *23*, 151 – 158.
[26] F. Cavani, N. Ballarini, A. Cericola, *Catal. Today* **2007**, *127*, 113 – 131.
[27] O. Czuprat, S. Werth, S. Schirrmeister, T Schiestel, J. Caro, *ChemCatChem* **2009**, *1*, 401 – 405.
[28] A. V. Gaikwad, V. Boffa, J. E. ten Elshof, G. Rothenberg, *Angew. Chem.* **2008**, *120*, 5487 – 5490; *Angew. Chem. Int. Ed.* **2008**, *47*, 5407 – 5410.
[29] R. Kreiter, M. D. A. Rietkerk, H. L. Castricum, H. M. van Veen, J. E. ten Elshof, J. F. Vente, *ChemSusChem* **2009**, *2*, 158 – 160.
[30] L. Bedel, A. C. Roger, C. Estournes, A. F. Sammels, *Catal. Today* **2003**, *85*, 207 – 218.
[31] M. C. Petri, B. Yildiz, A. E. Klickman, *Int. J. Nuclear Hydrogen Production and Application* **2006**, *1*, 79 – 91.
[32] J. D. Holladay, J. Hu, D. L. King, Y. Wang, *Catal. Today* **2009**, *139*, 244 – 260.
[33] R. M. Navarro, M. C. Sánchez-Sánchez, M. C. Alvarez-Galvan, F. del Valle, J. L. G. Fierro, *Energy Environ. Sci.* **2009**, *2*, 35 – 34.
[34] T. Schiestel, M. Kilgus, S. Peter, K. J. Caspary, H. H. Wang, J. Caro, *J. Membr. Sci.* **2005**, *258*, 1 – 4.

